

1 Supplementary Information

2 **Supplementary Methods**

3 *Cell culture methods*

4 Six independent Normal Human Urothelial (NHU) cell lines of finite (non-immortalised)
5 lifespan were used in this study. The cell lines were established as described [1] using
6 anonymous discarded tissue from renal transplant surgery, with UK NHS approval (REC
7 reference 99/095) from the Leeds East Research Ethics Committee. NHU cells were
8 propagated in Keratinocyte Serum-Free Medium containing bovine pituitary extract,
9 recombinant human EGF (KSFM) and additionally supplemented with 30ng/ml cholera toxin.
10 Following expansion, NHU cells were differentiated in the same medium supplemented with
11 5% adult bovine serum and CaCl₂ was added to elevate the [Ca²⁺] from 0.09 to 2 mM,
12 according to published methods [2]. Differentiated cultures of the six independent cell lines
13 were exposed to IFN γ (200U/mL, BioTechne #285-IF) for 7 days and medium was changed
14 every 48 hours. Urothelial mitotic-quiescence and differentiation was largely unaffected by
15 IFN γ -treatment and although there was a significant gain of *KRT6A* expression, there was no
16 significant loss of transitional epithelial markers and no other indicators of squamous
17 change (Supplementary Table 1).

18

19 *mRNA Analysis*

20 Total RNA was collected in TRIzol reagent (Invitrogen) and mRNA-sequencing was
21 performed using an Illumina NovaSeq 6000 generating 150bp paired-end reads (Novogene
22 UK, Cambridge, UK). All mRNA-sequencing data was deposited at GSE174244. Following

23 standard quality control, gene-level expression values in transcripts per million (TPM) were
24 derived against the Gencode v35 human transcriptome using kallisto v0.46.1 [3].
25 Differentially-expressed genes were identified using the sleuth v0.30.0 [4] implementation
26 of the likelihood ratio test (LRT), accounting for matched genetic backgrounds, generating
27 Benjamini-Hochberg corrected q-values. For volcano plots (performed in R v4.0.4
28 EnhancedVolcano v1.8.0), fold-change values used a $\log_2(\text{TPM}+1)$ transformation to reduce
29 the influence of low abundance transcripts. This analysis identified 107 genes that were
30 significantly ($q < 0.05$) >2-fold increased by IFN γ and 48 genes whose expression was
31 significantly ($q < 0.05$) more than halved by IFN γ -treatment of urothelial tissues
32 (Supplementary Table 1).

33

34 *Publicly-Available Bladder Cancer Cohort Data*

35 Patient data for four publicly-available bladder cancer cohorts was downloaded following
36 instructions in their relevant publications [5-8]. Two cohorts focussed on non-muscle
37 invasive bladder cancer (NMIBC) and from these we extracted only the T1 tumours for
38 further analysis [5, 7]. Two cohorts we of muscle invasive bladder cancer (MIBC) and from
39 these we extracted the tumours transcriptomically classified as the “Basal/Squamous”
40 subtype for further analysis based on the high variability in the IFN γ -Signature that we
41 observed in this group [6, 8, 9]. mRNA-sequencing data was remapped to Gencode v35
42 human transcriptome using kallisto v0.46.1 where possible [3]. MIBC gene array data from
43 the Lund cohort was utilised as deposited at GSE83586 to generate Combat centered probe
44 fluorescence values [8].

45

46 *IFN γ -signature generation*

47 All $q < 0.05$ significantly >2-fold IFN γ -increased genes were extracted from the TCGA-BLCA [6]
48 and UROMOL2021 [7] cohorts of MIBC and NMIBC, respectively. Genes regulated by IFN γ *in*
49 *vitro* can be regulated predominantly by other mechanisms in tissues and to refine the
50 signature, Spearman correlation matrices were calculated to compare all genes with one
51 another. The median Spearman Rho for each gene in comparison with all others was
52 calculated in each cohort. The median Spearman Rho values for the TCGA-BLCA and
53 UROMOL2021 cohorts were averaged and only genes with a value greater than 0.5 were
54 retained (n=33; gene list in Supplementary Table 2) to generate a transcriptomic classifier
55 relevant to both NMIBC and MIBC, where all genes were >2-fold increased by IFN γ *in vitro*
56 and closely related to one another in tumours.

57 Initial evaluation of the IFN γ -signature in tumours was performed on $\log_2(\text{TPM}+1)$ data using
58 hierarchical clustering (based on Euclidean distance and complete linkage. This approach
59 highlights the relationship between samples in the full cohorts of NMIBC UROMOL2021 [7]
60 (Supplementary Fig. 3) and MIBC TCGA-BLCA [6] (Supplementary Fig. 5).

61

62 *IFN γ -signature analysis*

63 mRNAseq data expressed as TPMs for tumours from the NMIBC cohorts was combined to
64 create one large cohort for analysis. For the MIBC cohorts, to allow integration of data
65 acquired by different methods (TCGA-BLCA mRNA-sequencing [6] with the Lund gene array
66 [8] data) each cohort was clustered separately into IFN γ -signature high and low groups.
67 Classification of tumours was performed on $\log_2(\text{TPM}+1)$ data using Euclidean distance k

68 means clustering into two groups of T1 NMIBC tumours (from the UROMOL2021 [7] and
69 Northwestern Memorial Hospital [5] cohorts) and Basal/Squamous classified [9] MIBC
70 tumours (TCGA-BLCA [6]). Classification of Basal/Squamous MIBC tumours from the Lund [8]
71 cohort was performed using Euclidean distance k means clustering into two groups on log-
72 transformed Combat centered probe fluorescence.

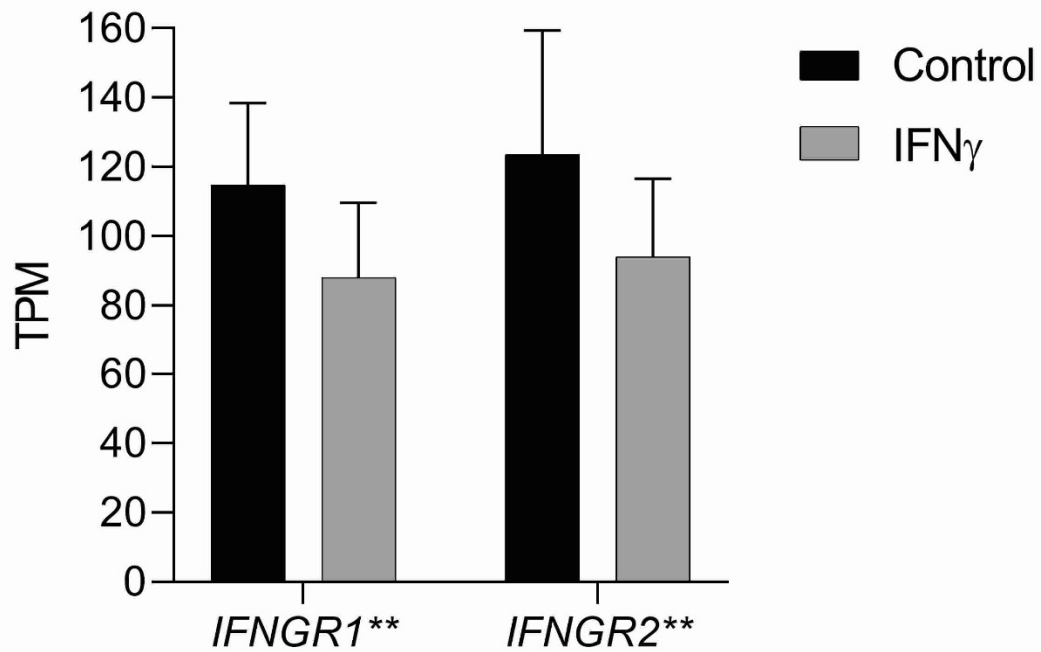
73 A single-value IFN γ -signature score was derived by unit-length scaling the $\log_2(\text{TPM}+1)$ data
74 (or log-transformed Combat centered probe fluorescence for the Lund cohort [8]) for each
75 gene. Unit-length scaled data for the genes in the signature were then summed on a per
76 patient basis before being re-scaled (again 0-1). This derived a single value IFN γ -signature
77 score that could be ranked to generate Spearman Rho values in comparison with ranked
78 gene expression values (eg *IFNG*) in the various cohorts. The single-value IFN γ -signature
79 scores for the combined T1, TCGA-BLCA and Lund cohorts are provided in Supplementary
80 Tables 3, 5 and 6, respectively.

81 Survival analysis was performed in Prism v9.3.1 (Graphpad). T1 NMIBC tumours and
82 Basal/Squamous classified MIBC tumours from the different cohorts were pooled to support
83 Kaplan-Meier NMIBC Recurrence Free Survival (RFS) and MIBC Overall Survival (OS) analysis,
84 respectively. Statistical significance of the difference between Kaplan-Meier curves for IFN γ -
85 signature high and low groups was performed using Mantel-Cox and Gehan-Breslow-
86 Wilcoxon tests, with hazard ratios calculated using both Mantel-Haenszel and log rank
87 approaches. A Cox proportional hazards regression analysis was performed using the pseudo-
88 continuous unit-length scaled IFN γ -signature scores to demonstrate that the effects of IFN γ -
89 signalling persist without dichotomising the tumours.

90

91 *TCGA-BLCA mutational signature analysis*

92 TCGA-BLCA legacy mutation data [6] was downloaded from cBioPortal [10]. The single base
93 substitution (SBS) signature for all tumours was analysed using the “Catalog” input for the
94 “signal” workflow for mutational signature analysis by comparison against the Catalogue of
95 Somatic Mutations In Cancer “COSMIC” reference SBS signatures common in bladder tumours
96 (namely SBS2, SBS4, SBS5 and SBS13; <https://signal.mutationalsignatures.com/> [11]).



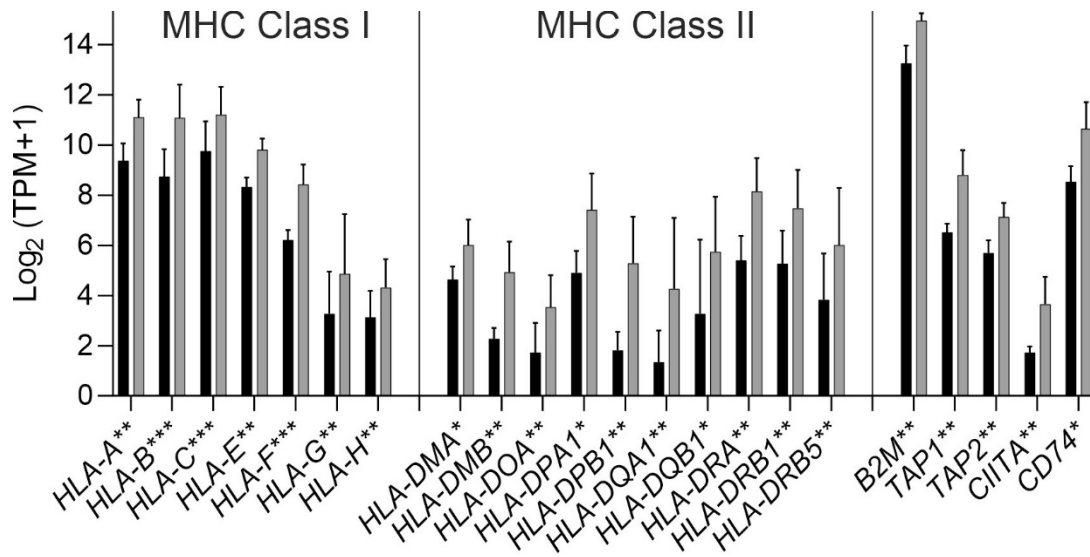
98

99 *Supplementary Figure 1 – Urothelial expression of both IFN γ receptor isoform genes was*

100 *high but significantly reduced by IFN γ treatment. Mean log₂ fold changes were -0.39 and -*

101 *0.38 for IFNGR1 and IFNGR2, respectively. Stars following gene names indicate significance*

102 ***=p<0.01.*



103

104

Supplementary Figure 2 – Gain in expression of a broad range of human leukocyte antigen

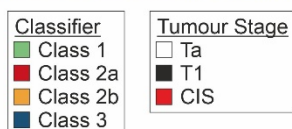
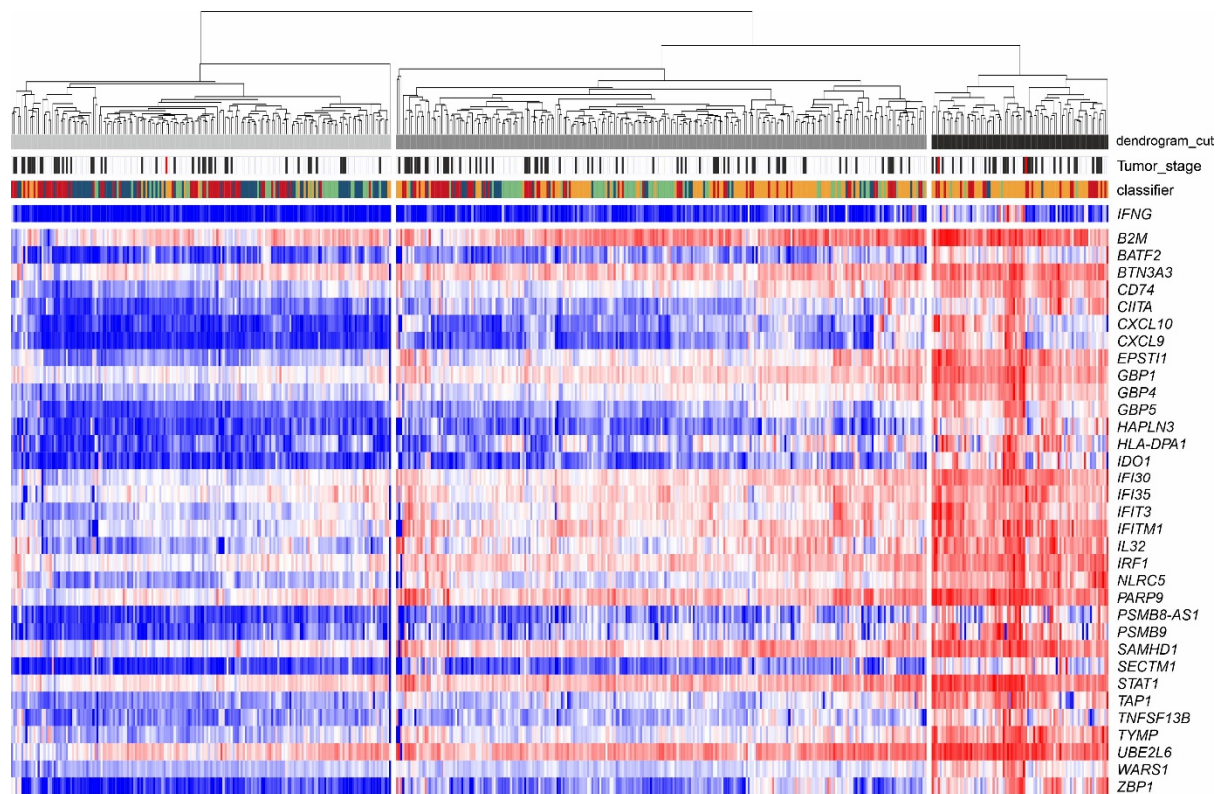
105

(HLA) genes. This study used cell derived from six independent donors. Stars following gene

106

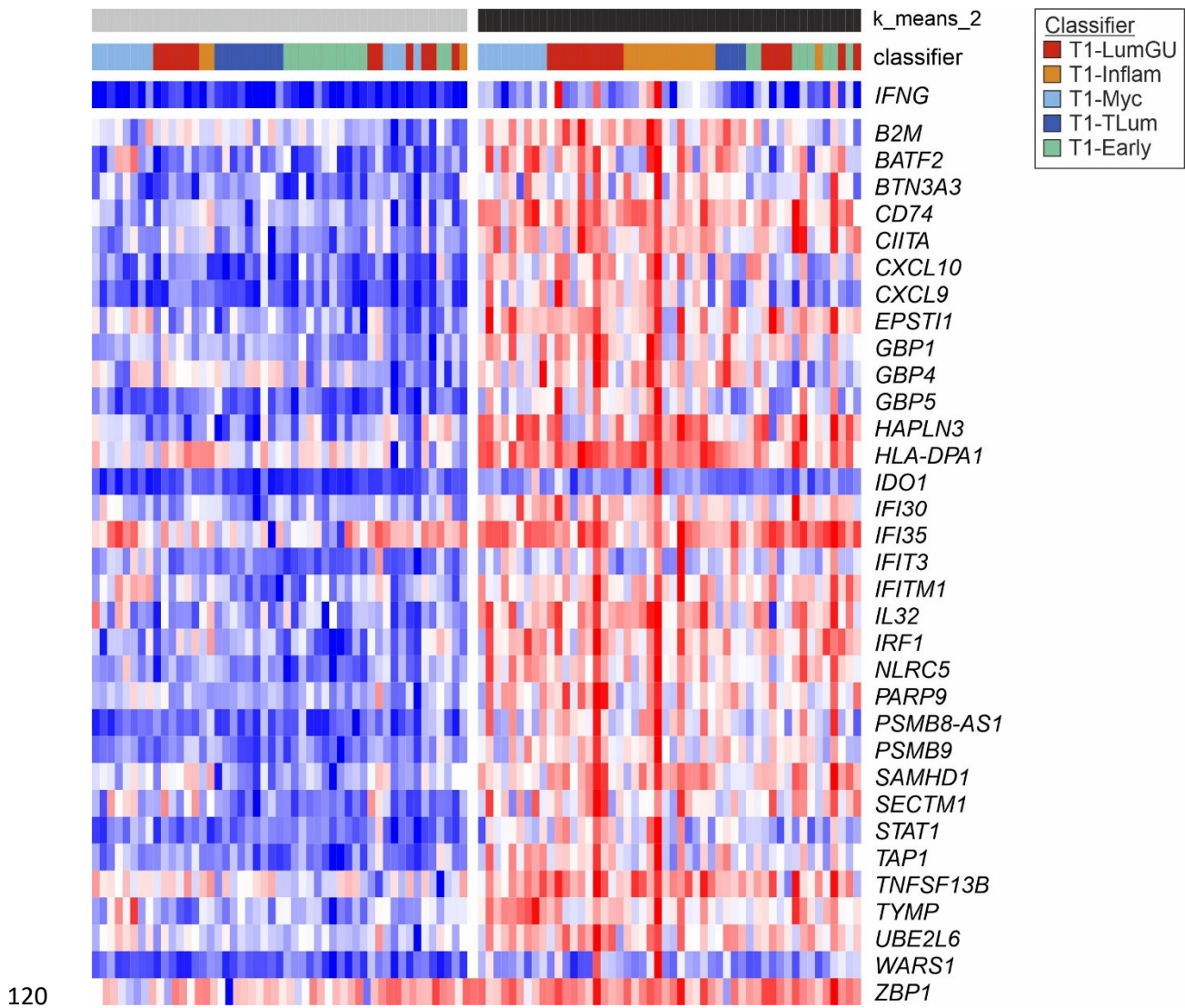
*names indicate >2-fold changes with significance *= $q < 0.05$, **= $q < 0.01$ and ***= $q < 0.001$.*

107

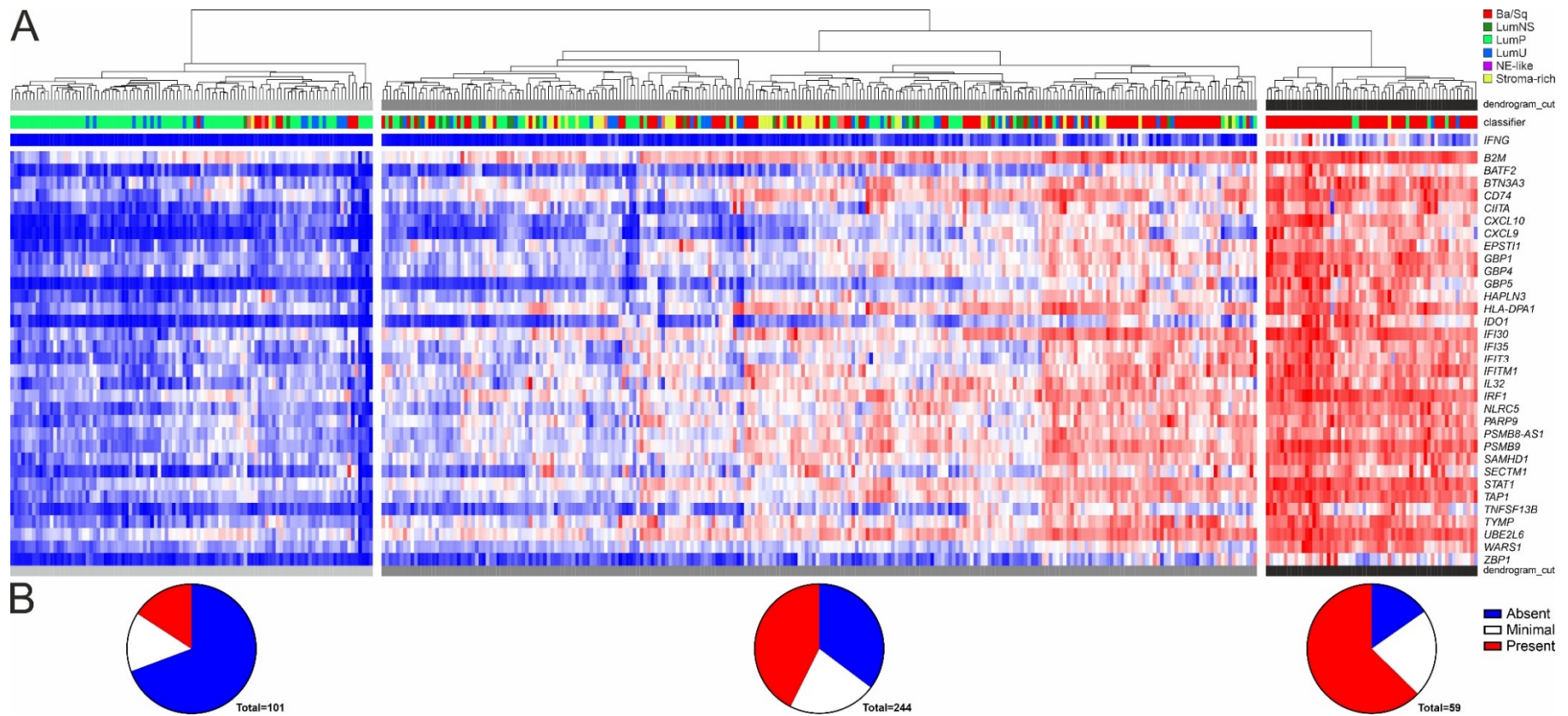


108

109 *Supplementary Figure 3 – The full UROMOL2021 NMIBC cohort (n=535; [7]) expression of the*
 110 *IFN γ -signature genes. Tumours were split using hierarchical clustering based on Euclidean*
 111 *distance with complete linkage. The IFNG gene is not part of the signature but is included*
 112 *above to show the lack of sensitivity when relying on IFNG transcript abundance alone. IFNG*
 113 *transcript abundance was significantly correlated with the IFN γ -signature (Spearman*
 114 *Rho=0.57; p=1.02x10⁻⁴⁶). Tumours are coloured according to the 2021 classification into four*
 115 *subtypes (Class 1, Class 2a, Class 2b and Class 3) [7]. The heatmap shows enrichment of IFN γ*
 116 *responsive gene expression in a subset of the Class 2b group of NMIBC. Lindskrog et al.*
 117 *identified Class 2b as being the most immune-infiltrated tumours [7]. Class 2a tumours were*
 118 *predominantly IFN γ -signature^{low} and had the highest recurrence rate in the original*
 119 *publication [7].*

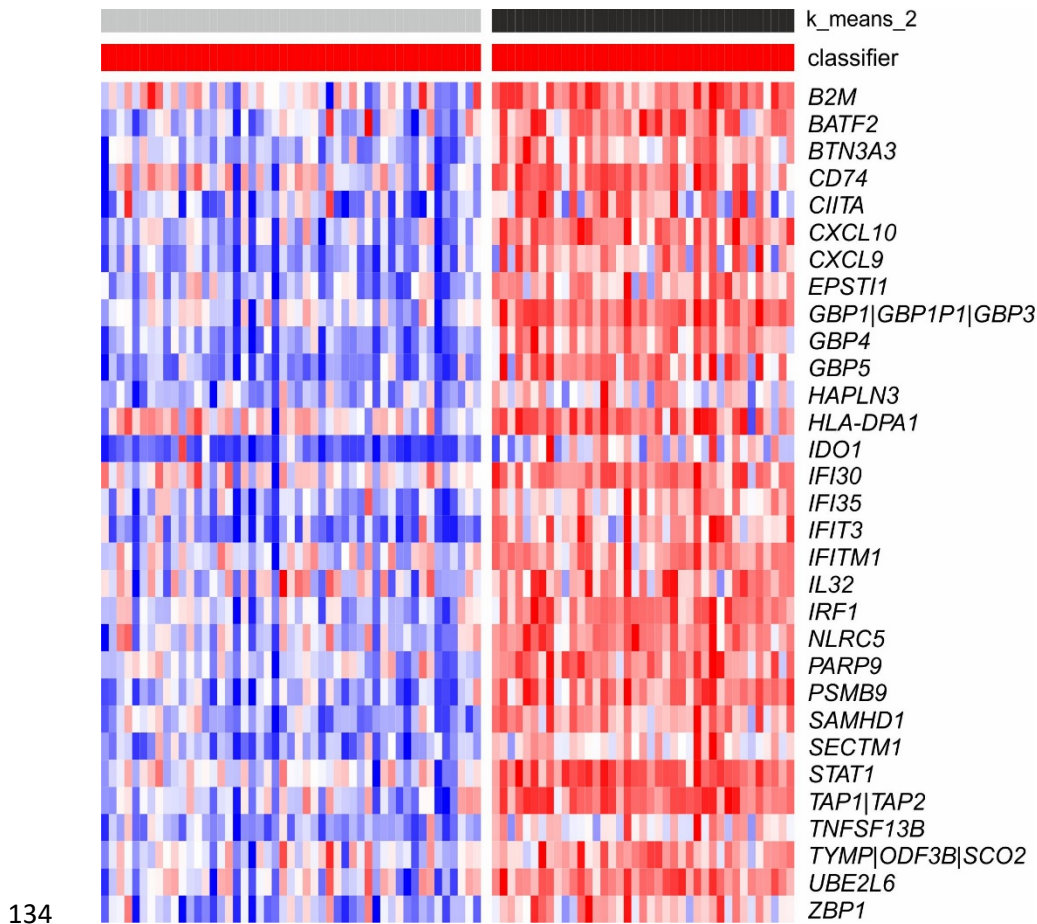


Supplementary Figure 4 – Heatmap and k means clustering based on expression of the IFN γ -signature in the T1 tumours of the Northwestern Memorial Hospital (NMH) cohort (n=99; shown with the classifier from the original report [5]). The IFN γ -signature shows a Spearman rank correlation of 0.67 ($p=1.66 \times 10^{-14}$) with the IFNG gene in this cohort.

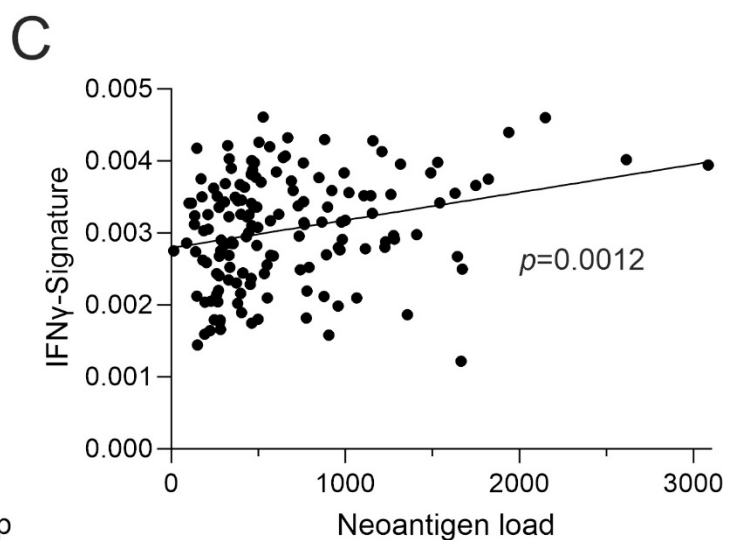
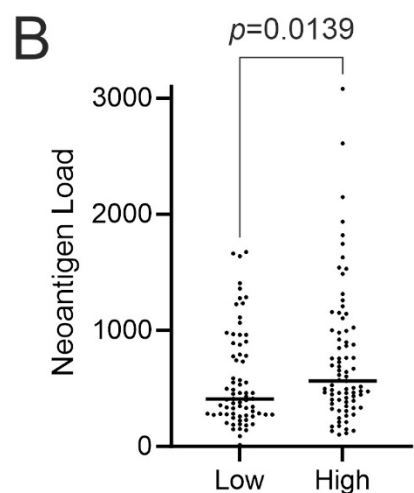
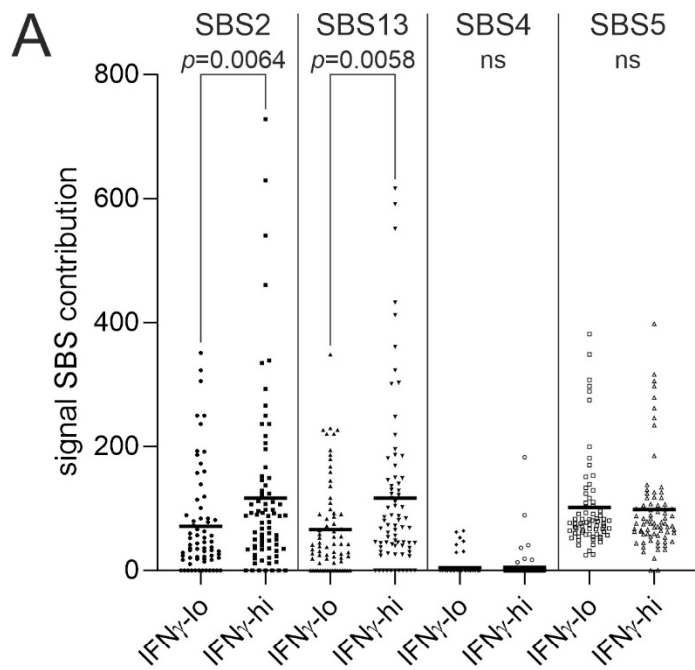


125

126 *Supplementary Figure 5 – (A) The full TCGA-BLCA MIBC cohort (n=404; [6]) expression of the IFN γ -signature genes. Tumours were split using*
 127 *hierarchical clustering based on Euclidean distance with complete linkage. The IFNG gene itself is not part of the signature and has a limited*
 128 *sensitivity for detecting IFN γ signalling; however, it does show significant correlation with the IFN γ -signature (Spearman Rho=0.83; p=2.86x10⁻¹⁰²).*
 129 *Tumours are coloured according to the 2019 consensus classification into six subtypes (Basal/Squamous, Luminal Non-specified, Luminal*
 130 *Papillary, Luminal Unstable, Neuroendocrine-like and Stroma-rich) [9]. The heatmap shows diversity in the IFN γ -signature within the*
 131 *Basal/Squamous group of MIBC and so these tumours were evaluated further (Figure 2C). (B) Histological grading of lymphocyte invasion of*
 132 *TCGA-BLCA tumours, showing significant (Chi square=56.63; df=4; p=1.48x10⁻¹¹) differences, including that IFN γ -signature low tumours were*
 133 *more likely to contain no lymphocytes.*



135 *Supplementary Figure 6 – Basal/Squamous classified tumours from the Lund MIBC cohort*
 136 *(n=88) showing expression of the IFN γ -signature genes (where present on the gene arrays*
 137 *employed). Multiple gene names indicate the gene array probes bind multiple targets. There*
 138 *was no specific probe for the IFNG gene and so correlation with the signature could not be*
 139 *calculated in this cohort.*



140

IFN γ -Signature K means Group

141

Supplementary Figure 7 – Basal/Squamous tumours of TCGA-BLCA have paired exome-

142

sequencing which allows the analysis of mutations. No significant over-mutation of

143

individual genes was observed in association with the IFN γ -signature. (A) However, APOBEC-

144

driven mutational processes had been significantly more active (as denoted by significant

145

enrichment of single base substitution signatures “SBS2” and “SBS13”) in tumours that

146

ultimately had higher IFN γ -signature scores. It was not the case that all mutational processes

147

were more active in forming tumours with a higher IFN γ -signature, as SBS4 and SBS5 were

148 *not enriched. Significance was analysed by Mann Whitney U test. ns = no significant*
149 *difference.*

150 *In silico analysis of the likely effects of mutations on neoantigen load in tumours was*
151 *previously described by TCGA consortium [6]. (B) Analysis of Basal/Squamous tumours of*
152 *TCGA-BLCA cohort showed a significantly higher predicted neoantigen load in the context of*
153 *higher IFN γ -signalling ($p=0.0139$). (C) Furthermore, linear regression analysis confirmed a*
154 *significant relationship between predicted neoantigen load and IFN γ -signature score*
155 *($p=0.0012$).*

156

157 **Supplementary References**

- 158 [1] Southgate J, Hutton KA, Thomas DF, Trejdosiewicz LK. Normal human urothelial cells in vitro:
159 proliferation and induction of stratification. *Lab Invest.* 1994;71:583-94.
- 160 [2] Cross WR, Eardley I, Leese HJ, Southgate J. A biomimetic tissue from cultured normal human
161 urothelial cells: analysis of physiological function. *Am J Physiol Renal Physiol.* 2005;289:F459-68.
- 162 [3] Bray NL, Pimentel H, Melsted P, Pachter L. Near-optimal probabilistic RNA-seq quantification. *Nat*
163 *Biotechnol.* 2016;34:525-7.
- 164 [4] Pimentel H, Bray NL, Puente S, Melsted P, Pachter L. Differential analysis of RNA-seq
165 incorporating quantification uncertainty. *Nat Methods.* 2017;14:687-90.
- 166 [5] Robertson AG, Groeneveld CS, Jordan B, et al. Identification of Differential Tumor Subtypes of T1
167 Bladder Cancer. *Eur Urol.* 2020;78:533-7.
- 168 [6] Robertson AG, Kim J, Al-Ahmadie H, et al. Comprehensive Molecular Characterization of Muscle-
169 Invasive Bladder Cancer. *Cell.* 2017;171:540-56 e25.
- 170 [7] Lindskrog SV, Prip F, Lamy P, et al. An integrated multi-omics analysis identifies prognostic
171 molecular subtypes of non-muscle-invasive bladder cancer. *Nat Commun.* 2021;12:2301.
- 172 [8] Sjobahl G, Eriksson P, Liedberg F, Hoglund M. Molecular classification of urothelial carcinoma:
173 global mRNA classification versus tumour-cell phenotype classification. *J Pathol.* 2017;242:113-25.
- 174 [9] Kamoun A, Reynies A, Allory Y, et al. A Consensus Molecular Classification of Muscle-invasive
175 Bladder Cancer. *Eur Urol.* 2019.
- 176 [10] Cerami E, Gao J, Dogrusoz U, et al. The cBio cancer genomics portal: an open platform for
177 exploring multidimensional cancer genomics data. *Cancer Discov.* 2012;2:401-4.
- 178 [11] Degasperi A, Amarante TD, Czarnecki J, et al. A practical framework and online tool for
179 mutational signature analyses show intertissue variation and driver dependencies. *Nature Cancer.*
180 2020;1:249-63.

181